

$\text{Li}^7(p,n)$, $(p,p'\gamma)$, and (p,γ) Reactions near Neutron Threshold*

H. W. NEWSON, R. M. WILLIAMSON, K. W. JONES,† J. H. GIBBONS,‡ AND H. MARSHAK§
Physics Department, Duke University, Durham, North Carolina

(Received August 5, 1957)

The $\text{Li}^7(p,n)$ total cross section has been measured in detail from threshold to 2.5-Mev proton energy. Between 1.88 and 1.92 Mev the cross section follows the equation for a very broad 2^- resonance and for s -wave particles: $\sigma_{pn} = (5/2)\pi\lambda^2 x / (1+x)^2$, where $x = \Gamma_n / \Gamma_p = 1$ at 50 kev above threshold. The remainder of the cross section up to 2.35 Mev is fitted by this level and the 3^+ level at 2.25 Mev. The neutron reduced width exceeds that of the proton by a factor of about five for both the 2^- and 3^+ levels; this is surprising for the self-mirror nucleus Be^8 . A small dip is observed just above neutron threshold in the yield of 478-kev gamma rays from $\text{Li}^7(p,p'\gamma)$. The shape of these data support the assumption of the broad 2^- neutron producing resonance with $\Gamma_p > 0.5$ Mev.

No anomaly is observed in the yield of Li capture gamma rays at neutron threshold; the 2.10-Mev resonance in this reaction (which probably is due to a 3^+ level) yields mainly 16-Mev gamma rays leading to the 2.9-Mev 2^+ level in Be^8 . The ratio of 16 to 19 Mev gamma rays is $\frac{2}{3}$ at both 1.7- and 2.5-Mev proton energy. The behavior of the $\text{Li}^7(p,n)$ extrapolated threshold was calculated as a function of target thickness and proton energy spread; shifts in the extrapolated thresholds and the distances between them and true threshold were less than one kev. The extrapolated threshold of a $\frac{1}{2}$ -kev target taken with a proton energy spread of 1 kev was observed to be $\frac{1}{2}$ kev lower in proton energy than a thick-target threshold.

I. INTRODUCTION

BECAUSE of the use of the $\text{Li}^7(p,n)$ reaction as a source of neutrons and as a calibrating reaction for accelerators, it is important to understand the reaction as well as possible, particularly near threshold. For this reason the total cross section has been re-measured in more detail than has been done previously,^{1,2} the competing $(p,p'\gamma)$ and (p,γ) reactions have been studied, and an attempt has been made to analyze the levels of the compound nucleus Be^8 , even though its level structure at an excitation energy of 19 Mev is much more complex than cases usually studied in nuclear spectroscopy. Further, the relation between true (p,n) threshold and extrapolated thresholds was studied as a function of proton energy spread and target thickness.

Adair has analyzed the (p,n) total cross section³ and neutron polarization⁴ and found that the resonance at a proton energy of 2.25 Mev can be 3^+ and that at least one wide level formed by s -wave protons must exist near threshold. Hanna² has measured the $\text{Be}^7(n,p)$ cross section with thermal neutrons and suggested a narrow s -wave level just below threshold. A 350-kev wide resonance has been observed^{5,6} in the $\text{Li}^7(p,\gamma)$ reaction at a proton energy of about 2.1 Mev. No resonances were seen in $\text{Li}^7(p,p')$ data⁷ in which protons were observed at an angle of 164° . Interference effects

which are probably due to the 2.1- and the 2.25-Mev resonances are seen in proton elastic scattering data;⁸ an anomaly is also observed at neutron threshold in these data. We wished to try to find out which of the above resonances were involved in neutron production.

II. $\text{Li}^7(p,n)$ REACTION

The energy and homogeneity of protons from a Van de Graaff accelerator were defined by a one-meter radius electrostatic analyzer. A very thin natural lithium target was evaporated, and its equivalent thickness^{||} found to be less than one kev by means of the neutron cross section apparatus described by Gibbons.⁹ We have found that an observed transmission ratio less than 50% (one-cm sample) at the 12.5-kev bismuth resonance shows that the neutron energy spread due to the lithium target thickness is less than one kev. The neutron detector consisted of a triangular lattice of BF_3 counters, which were 1 in. in diameter and 2 in. from center to center in a paraffin moderator. The counters were filled to 120-cm pressure with enriched BF_3 . The lithium target was located 12 in. within the paraffin moderator and the proton beam entered through an aluminum tube 1 in. in diameter with its axis parallel to the axes of the BF_3 counters; very few neutrons escaped from the lattice through this small hole. A graphite rod 1 in. in diameter and 4 in. long was placed against the target backing so that the forward neutrons emitted by the target near neutron threshold were scattered nearly isotropically.

Figure 1 shows a total yield curve for the (p,n) reaction against the proton energy. The solid dots are based on relative yield measurements made in this laboratory, the bars being the absolute Mn bath measurements of Taschek and Hemmendinger. (Data recently taken by Macklin and Gibbons¹⁰ show the

* This work was supported by the U. S. Atomic Energy Commission.

† Now at Department of Physics, Columbia University, New York, New York.

‡ Now at Oak Ridge National Laboratory, Oak Ridge, Tennessee.

§ Now at Brookhaven National Laboratory, Upton, New York.

¹ R. F. Taschek and A. Hemmendinger, *Phys. Rev.* **74**, 373 (1948).

² R. C. Hanna, *Phil. Mag.* **46**, 381 (1955).

³ R. K. Adair, *Phys. Rev.* **96**, 709 (1954).

⁴ A. Okazaki, *Phys. Rev.* **99**, 55 (1955).

⁵ P. C. Price, *Proc. Phys. Soc. (London)* **A67**, 849 (1955).

⁶ Swann, Rothman, Porter, and Mandeville, *Phys. Rev.* **98**, 1183(A) (1955).

⁷ S. Bashkin and H. T. Richards, *Phys. Rev.* **84**, 1124 (1951).

⁸ P. R. Malmberg, *Phys. Rev.* **101**, 114 (1956).

^{||} Note.—The thickness for 1.9-Mev protons.

⁹ J. H. Gibbons, *Phys. Rev.* **102**, 1574 (1956).

¹⁰ R. L. Macklin and J. H. Gibbons, *Phys. Rev.* (to be published).

same shape and a slightly higher absolute cross section.) The comparison of our uncorrected data with the Mn bath data indicated that our neutron counting arrangement was slightly energy-dependent. The departure from constant efficiency, about 15% over the range of measurement, was assumed to be linear with neutron energy, and this correction has been made to the solid dots in Fig. 1.

The solid lines in Fig. 1 represent an attempt to account for the neutron yield assuming only two resonances with Breit-Wigner shapes and the following approximate parameters: $E_0 = 1.9$ Mev, $l_p = l_n = 0$, $J^\pi = 2^-$, $g = \frac{5}{8}$, $\Gamma_n E_n^{-1/2} / \Gamma_p E_p^{-1/2} = C = 6$, $\Gamma_n = \Gamma_p$ when $E_p = 1.93$ Mev, and $(E_p - E_0)^2 / \Gamma_p^2 \ll 1$ for the resonance responsible for the lower curve in Fig. 1; and $E_0 = 2.25$ Mev, $l_p = l_n = 1$, $J^\pi = 3^+$, $g = \frac{7}{8}$, $\Gamma_n = \Gamma_p = 110$ kev at resonance, and $\Gamma_n E_n^{-1/2} (1 + \gamma_n^2) / \Gamma_p E_p^{-1/2} (1 + \gamma_p^2) = C = 7.5$. Here $\gamma = kR$, where R is the nuclear radius and k is the wave number of the particle in the center-of-mass

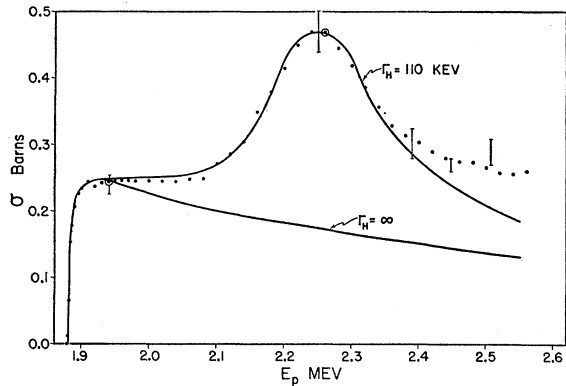


FIG. 1. The solid circles are the Li⁷(*p*, *n*) total yields reported in this paper; the vertical bars are the absolute yield measurements of reference 1. The lower solid curve is the calculated yield from a wide 2⁻ *s*-resonance and the upper solid curve is the calculated yield of the 2⁻ resonance added to a 3⁺ *P*-resonance. (See Sec. II.)

system; all other energies are in the laboratory system. $g = (2J+1) / [(2I+1)2]$, where J and I are the spins of compound nucleus and Li⁷, respectively. The approximate ratio of neutron to proton reduced width, C , was treated as a free parameter in fitting the data. When Coulomb effects and the level shift¹¹ (Δ) are considered, the shape of the calculated curves are little effected; however, the actual ratios of reduced widths¹¹ (γ_n^2 / γ_p^2) are 4.5 and 5.5 for the 1.9- and 2.25-Mev level, respectively.

The angular momentum and parity assignments for the 2.25-Mev level are those assumed by Adair.³ The partial widths for alpha, inelastic proton, and gamma emission are assumed to be negligible from both levels for the following reasons: Alpha emission should be forbidden by spin and parity consideration. Inelastic protons going to the $\frac{1}{2}^-$ 478-kev level of Li⁷ need two

¹¹ T. Teichmann and E. P. Wigner, Phys. Rev. **87**, 123 (1952).

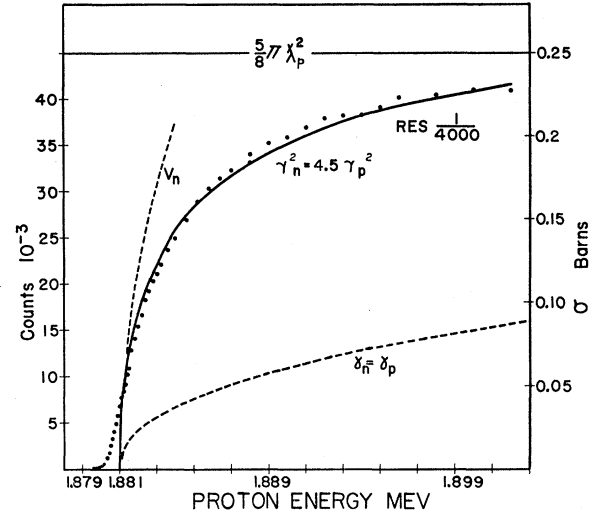


FIG. 2. The solid circles are measured Li⁷(*p*, *n*) total yields taken with a target less than one kev thick. The upper dashed curve represents a yield proportional to center-of-mass neutron velocity. The solid curve and the lower dashed curve are calculated yields from a wide 2⁻ *S*-resonance with the two different values of γ_n^2 / γ_p^2 shown.

more units of angular momentum than do the ground state protons and neutrons for both the 2⁻ and 3⁺ levels. The (*p*, *p'*) and (*p*, γ) cross sections are small compared to the (*p*, *n*) and (*p*, *p*) cross sections.¹²

The lower curve in Fig. 1 was calculated from the equation:

$$\sigma_{pn} = (5/8)\pi\lambda_p^2 4x / [(1+x)^2 + 4(E_p - E_0)^2 / \Gamma_p^2]. \quad (1)$$

Here $x = \Gamma_n / \Gamma_p = C(E_p - E_t)^{1/2} / E_p^{1/2}$ and $E_t = 1.881$ Mev; the second term in the denominator of Eq. (1) is neglected. C was adjusted to account for the rapid rise near threshold and the maximum in the lower curve 50 kev above threshold. It is seen that the broad 2⁻ level will account for all of the yield up to 1.92 Mev and most of the background underneath the 2.25-Mev level. The two resonances are insufficient to account for the yield above 2.4 Mev. Further, if Γ_p is finite, the calculated cross section should be lower at the higher energies.

Figure 2 shows more detailed total cross section data near threshold taken with a proton energy spread of $\frac{1}{2}$ kev. (Data taken with a proton spread of $\frac{1}{4}$ kev were essentially the same.) The calculated Doppler spread due to thermal motion of the target atoms was 400 ev. Thus, the effective beam spread was about 600 ev and the target thickness was less than 1 kev. The location of true threshold was obtained by comparison with the calculations shown in Figs. 6 and 7. The fit is not very sensitive to the choice of C , which is 6 ± 1 . This uncertainty is judged from the latitude in fitting the data and the possible neutron energy dependence of the neutron detector.

¹² F. Ajzenberg and T. Lauritsen, Revs. Modern Phys. **27**, 77 (1955).

The curve labeled v_n in Fig. 2 indicates a yield proportional to center-of-mass neutron velocity; this would be expected if s -wave neutrons are produced and there is no nearby resonance. The fact that the data rise less rapidly than v_n can be explained by assuming a narrow resonance just below threshold,² but this does not explain the data over a wide energy region nor does it agree with our $\text{Li}(p,p'\gamma)$ data (see Sec. III). The lower dashed curve in Fig. 2 is the calculated contribution of a broad 2^- resonance obeying Eq. (1) and having $\gamma_n = \gamma_p$. The addition of a similar 1^- level would account for only 60% of the observed cross section. It is, of course, possible to assume both a 2^- and a 1^- level with values of (γ_n^2/γ_p^2) less than 4.5 and fit the magnitude of the cross section at 1.92 Mev, but the over-all fit would not be as good. Further, a 1^- level could contribute s -wave inelastic protons and the data in Sec. III indicate a very small effect which is more in keeping with a 2^- level giving d -wave inelastic protons.

As a further test of Eq. (1), we calculate the thermal $\text{Be}^7(n,p)$ cross section with the aid of the reciprocity law:

$$\sigma_{np} = (5/8)\pi\lambda_n^2 4x/(1+x)^2 = 45\,000 \text{ barns.} \quad (2)$$

This is in reasonable agreement with $50\,000 \pm 8000$ barns—the average of Hanna's value of $\text{Be}^7(n,p)$ and Be^7 destruction cross sections.² This calculation assumes that Be^7 has a spin of $\frac{3}{2}$, and the agreement can be taken as support for this assumption.

One might expect that levels of the self-mirror nucleus Be^8 would have $\gamma_n = \gamma_p$, but the following arguments tend to confirm our assumptions. When one uses our data or those of Macklin and Gibbons, the resonance at 2.25 Mev cannot be fitted by a 3^+ level having $\gamma_n = \gamma_p$ even if the highest possible flat background is assumed underneath it.¹⁰ Adair³ has suggested that two interfering levels having isotopic spins 0 and 1 might account for the large cross section near threshold. We have tried all possible combinations of two interfering s -wave levels having $\gamma_n = \gamma_p$ and found that the (p,n) data deviate from these calculations by factors that are large compared to experimental errors. Also, the close approach of the $\text{Li}(p,n)$ cross section to $(5/8)\pi\lambda_p^2$ at 1.93 Mev, the good fit near threshold, and the calculated agreement with the $\text{Be}(n,p)$ cross section support the assumption of compound nucleus formation and unequal γ_n and γ_p . More accurate absolute (p,n) and (n,p) cross sections would be of interest; but at present, the evidence for unequal neutron and proton reduced widths in Be^8 appears to be rather strong.

III. $\text{Li}^7(p,p'\gamma)$ AND $\text{Li}^7(p,n'\gamma)$

A lithium target 5 kev thick was bombarded by electrostatically analyzed protons. Pulses from a 2×2 in. NaI(Tl) scintillation counter were amplified and recorded by a ten-channel analyzer. The shape of the pulse height spectrum of the 478-kev gamma rays from

the $\text{Li}^7(p,p'\gamma)$ reaction was carefully recorded below the $\text{Li}^7(p,n)$ threshold. Above threshold this shape was superimposed on the pulse height spectrum of approximately 8-Mev gamma rays due to neutron capture in NaI. The shape of this capture gamma spectrum was studied by putting paraffin around the NaI, placing this counter at zero degrees, and setting the proton energy just above threshold so that neutrons were bunched in the forward direction. Under these conditions the capture gamma spectrum was much more intense than the 478-kev gamma spectrum. Photopeak yields of the 478-kev gamma are plotted as a function of proton energy in Fig. 3. The size of the neutron and machine background correction which was made to the top curve is shown. The counter was at 120° with respect to the incident proton beam. The upper curve corresponds to a relative total inelastic scattering cross section up to 2.4 Mev; above the threshold for $\text{Li}^7(p,n'\gamma)$, 430-kev γ rays are also counted. The gamma rays should be isotropic since they are emitted by $J = \frac{1}{2}$ levels at 478 kev in Li^7 and at 430 kev in Be^7 . We measured angular distributions at proton energies of 1.7, 2.0, 2.6, and 3.0 Mev and found them to be isotropic.

The most interesting feature of Fig. 3 is the dip observed in the gamma-ray yield above the (p,n) threshold energy. This dip is shown in more detail in the inset and the counting statistics given apply only to that limited energy region. The counter background increases sharply at 1.92 Mev, the threshold for neu-

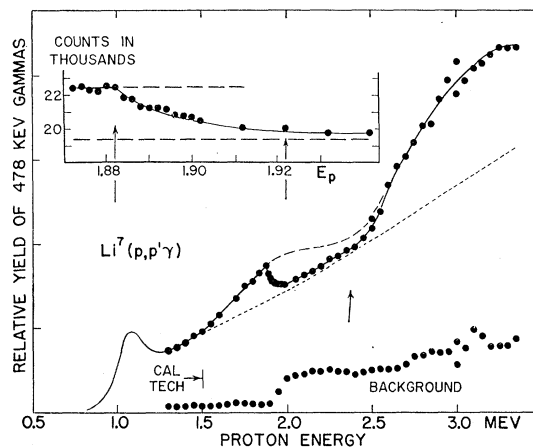


Fig. 3. The upper solid circles and solid line up to 2.4 Mev represent the yield of 478-kev gammas from the $\text{Li}^7(p,p'\gamma)$ reaction corrected for counter background, which is shown by the lower solid circles. The gamma counter angle with respect to the incident beam was 120° . The upper dashed line indicates the possible contribution of a broad level if the effect of the opening neutron channel is absent. The inset shows the data and the calculated effect above threshold of the opening neutron (2^-) channel. The dotted line is the approximate inelastic scattering cross section after subtracting the effects of the low-energy neutron group and the 2^- level. The vertical arrows indicate the thresholds for the two neutron groups. The absolute cross section at the threshold for $\text{Li}^7(p,n'\gamma)$ is about 80 mb if our data are normalized to those of Kraus¹¹ (labeled "Cal. Tech").

trons in the backward direction. Therefore, the dip in the net gamma-ray yield at 1.88 Mev is not the result of improper background subtraction.

If one assumes that a broad 2⁻ level produces most of the neutrons at threshold and the small fraction of the (*p*, *p'*γ) yield shown above the dotted line in Fig. 3, then the dip is the result of the increase of Γ_n in the denominator of the simple single-level Breit-Wigner formula for $\sigma_{pp'}$. We have assumed that $\sigma_{pp'}$ has a constant numerator and the same denominator as Eq. (1) and have calculated the shape of the dip shown by the solid line in the inset of Fig. 3. The background underneath the 2⁻ resonance was assumed to be straight, and the size of the dip was adjusted to fit the experimental points at 1.88 and 1.92 Mev.

The simple Breit-Wigner formula neglects the effect below neutron threshold of the neutron channel on the (*p*, *p'*) reaction. When closed channels are not neglected, an anomaly will generally be seen both below and above threshold.¹³ However, if one is considering a single resonance and no interference terms, then the size of a cross section may still only decrease above the threshold of the competing channel.¹⁴ This appears to be true of our (*p*, *p'*γ) data. When there are interference terms, the cross section is generally affected on both sides of threshold.¹⁴ Malmberg's Li⁷(*p*, *p*) data⁸ appear to show this at 1.88 Mev. The anomaly is presumably due to the broad 2⁻ resonance and not the 2.1-Mev resonance (Sec. IV).

Figure 3 shows no sign of a narrow resonance below the dip at 1.88 Mev. The data suggest that the neutron-producing resonance has $\Gamma_p > 0.5$ Mev. The maximum allowed proton width¹² for a single, particle level would be about 7 Mev. Since the reduced neutron width should not exceed the Wigner limit and $\gamma_n^2/\gamma_p^2 = 4.5$, $0.5 < \Gamma_H < 7/4.5 = 1.5$ Mev; $\gamma_n^2 > \frac{1}{3}$ the Wigner limit; and $\gamma_p^2 > 0.07$ of the limit.

The contributions of resonances at 2.1 or 2.25 Mev are evidently small. This is consistent with spin assignments $\geq 2^-$ or 3^+ which require that the outgoing inelastic proton orbital angular momenta be greater than one. Figure 3 has been corrected, approximately, for the contributions of 430-keV gamma rays with the help of preliminary Li(*p*, *n'*) data taken in this laboratory. The dotted line above 2.4 Mev is the roughly corrected inelastic scattering cross section. Note that the yield of low-energy neutrons rises rather rapidly near threshold. A wide ($\Gamma = 1-2$ Mev) resonance at 3 Mev or higher could account for most of the inelastic scattering in Fig. 3 and also for the low-energy neutrons. A neutron emitting resonance of about this description is also necessary to account for part of the neutron yield in Fig. 1 above 2.35 Mev. A 1⁻ level or an *l*=1 (1⁺) level as suggested by Macklin and Gibbons¹⁰ would be favorable to the emission of both neutrons

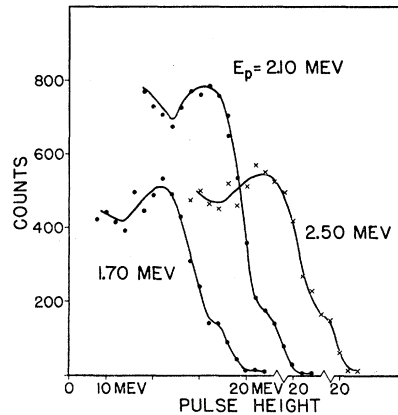


Fig. 4. Pulse height spectra in a 2×2 in. NaI(Tl) detector due to the Li⁷(*p*, γ) reaction. The abscissa is broken so that the three curves are not superimposed.

groups and also of inelastically scattered protons. A more positive identification of the proposed 1[±] level may result from current measurements on the low-energy neutron group.

IV. Li⁷(*p*, γ) REACTION

The target and detector are described in Sec. III. The weak 19- and 16-Mev capture gamma rays¹² from Li⁷(*p*, γ) were partially resolved as seen in Fig. 4. At proton energies above the Li(*p*, *n*) threshold, neutrons again caused copious capture gamma rays in the NaI detector. We investigated very carefully the counting rates for these capture gamma rays which would give sufficient pile-up pulses to distort the Li(*p*, γ) spectrum above 10 Mev. Counting rates were then kept low enough to avoid this. The spectra in Fig. 4 show that the increased yield at 2.1-Mev proton energy is not due to pile-up pulses. They further indicate that most, if not all, of the increase is due to the 16-Mev gammas which go to the 2.9 Mev 2⁺ level¹² in Be⁸, rather than to the 19-Mev gammas to the 0⁺ ground state. This fact suggests that the 2.1-Mev resonance is 2⁻, 3⁺, 3⁻, 4⁺ on the basis of the multipolarities required for the two capture gamma rays.

More detailed yields of the combined 19- and 16-Mev gamma rays were taken at counter angles of 0° and 90° with respect to the proton beam in order to look for an anomaly at neutron threshold (Fig. 5). The dashed line indicates the total capture cross section predicted by the simple Breit-Wigner formula if $E_0 = 2.13$ Mev, $\Gamma_p = 100$ kev, and (Γ_n/Γ_p) has the same values that were used in Eq. (1). It is seen that the increase of Γ_n at threshold only causes a slight change of slope in the curve. The assumption of $\gamma_n = \gamma_p$ would only make the change less pronounced. Therefore, it is possible that the 2.1-Mev resonance has an appreciable neutron partial width so far as we can tell from Fig. 5. However, the 2.1-Mev peak in Malmberg's⁸ approximate total elastic scattering curve indicates $\sigma_0 \approx 4\pi\lambda_p^2$,

¹³ E. P. Wigner, Phys. Rev. 73, 1002 (1948).

¹⁴ R. K. Adair (private communication).

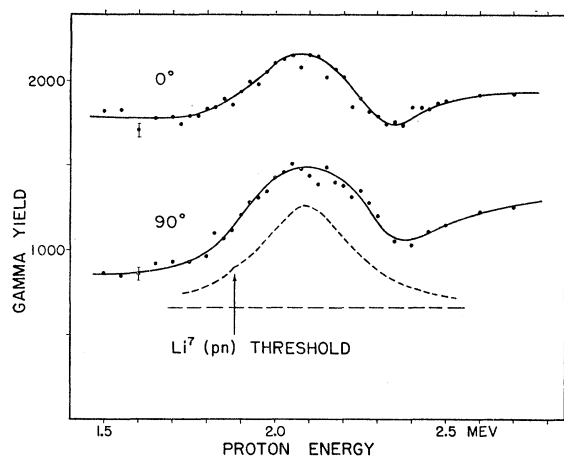


FIG. 5. $\text{Li}^7(p,\gamma)$ yields taken at 0 and 90° with the NaI(Tl) detector integral bias set for 10-Mev pulses. The dashed curve indicates the total cross section calculated by the simple Breit-Wigner formula with $E_0=2.13$ Mev, $\Gamma_p=100$ kev, and $(\gamma_n/\gamma_p)^2=4.5$.

and hence $\Gamma_p \gg \Gamma_n$; this is in agreement with our failure to observe any effect from this resonance in the neutron yield curve. The absence of a dip at 1.88 Mev does not indicate that the broad 2^- level does not contribute capture gamma rays. An interference dip is seen to the right of the 2.1-Mev resonance in Fig. 5; therefore, the total width of the level is probably greater than 350 kev. If one considers the Wigner limit¹¹ for proton widths, l_p should be less than 3. This makes the level assignment 4^+ unlikely. Malmberg has pointed out that the apparent interference of the 2.25- and the 2.1-Mev levels observed in the proton elastic scattering data at 90° indicates that the 2.1-Mev level must have odd l_p if the 2.25 level has odd l_p .¹² This and our observations would make the 2.1-Mev level seem to be 3^+ . On this basis we must assume $\gamma_n^2/\gamma_p^2 \leq 1$ in order to explain a low neutron emission from a 3^+ level; from the point of view of neutron emission 3^- is the most attractive assignment and 2^- the least.

Wilkinson¹⁵ has suggested that the nonresonant $\text{Li}(p,\gamma)$ radiation in this proton energy region may be mostly due to a direct reaction involving s -wave protons and $E1$ gamma rays. The rather large off-resonance anisotropy seen in Fig. 5 shows that higher angular momenta are important and that the further analysis of the differential cross section would be difficult. The ratio of 16- to 19-Mev gammas is approximately $\frac{2}{3}$ in the nonresonant regions of 1.7 Mev, and 2.5 Mev (Fig. 4). Wilkinson's analysis predicts $\frac{7}{2}$ for L - S coupling and $\frac{3}{2}$ for j - j coupling.

¶ Note added in proof.—Preliminary results of a phase shift analysis of $\text{Li}(p,p)$ data by J. Olness indicate that the interference just discussed may be due to a 3^- level at 2.1 Mev interfering with the broad 2^- level and the 3^+ level at 2.25 Mev interfering with a wide 1^+ level at about 3 Mev. We now conclude that 3^- is the most likely assignment for the 2.1-Mev level and 1^+ for the wide level near 3 Mev.

¹⁵ D. H. Wilkinson, *Phil. Mag.* **45**, 259 (1954).

V. $\text{Li}^7(p,n)$ THRESHOLD AND EXTRAPOLATED END POINTS

Nuclear reaction thresholds are usually taken as a linear extrapolation to zero product-particle yield. We call this an extrapolated threshold, as distinguished from the true threshold, at which the product particle has zero energy in the center-of-mass system for a proton of average energy striking the surface of the target. This is the only possible definition of true threshold for a target so thick that some of the protons are slowed below threshold before traversing the target. The relationship between the true neutron threshold for the $\text{Li}^7(p,n)$ reaction and the extrapolated threshold is of interest when one wishes to know the energy of the reaction very accurately. Further, since the thick-target extrapolated threshold is now quoted with an accuracy of ± 0.5 kev,¹⁶ one would like to know how sensitive this point is to target thickness and incident beam resolution. The good fit to the $\text{Li}(p,n)$ total cross section we have obtained allows us to study the above questions. The calculated curves shown in Figs. 6, 7, and 8 were obtained by simple graphical integration of Eq. (1).

Figure 6 shows how several assumed triangular incident beam spreads modify the neutron yield from a target of zero thickness. Most interesting is the fact that extrapolated thresholds depend on the incident beam resolution and are at lower average proton energies than true threshold.

Figure 7 shows the calculated effect of target thickness on the neutron yield when the incident beam is assumed to have no energy spread. Here, the extrapolated thresholds lie above the true threshold energy. A thick-target extrapolation is about 400 ev above true threshold.

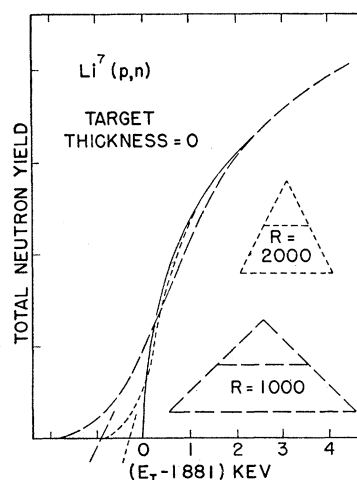


FIG. 6. Calculated modifications of the thin-target $\text{Li}^7(p,n)$ total yield due to various assumed triangular incident beam energy spreads.

¹⁶ Jones, Douglas, McEllistrem, and Richards, *Phys. Rev.* **94**, 947 (1954). Other absolute threshold references are given.

Figure 8 shows the calculated thick-target yield curve. The incident beam spread was chosen to approximate the Doppler effect one gets when one uses the singly charged molecular hydrogen beam. This effective energy spread due to the internal motion of protons in the molecular ion is about 1/500;¹⁷ we have repeated these data and found the same effective energy spread. Figure 8 shows that the thick-target extrapolated threshold is not shifted if the fillet due to beam spread is properly recognized; this is true for any type of energy spread of the incident beam.

The absolute measurements of the Li(*p*,*n*) threshold¹⁶ were thick target extrapolated thresholds. The regions of extrapolation used were in the order of 2 to 10 kev. Since neutrons were only counted in the forward direction¹⁶ and since the forward cone of neutrons has opened to 30° at 10 kev above threshold, an exact comparison of data with the calculated total cross section is impractical. In practice, the region of extrapolation should be larger than the beam energy spread and smaller than the energy above threshold at which the neutron cone is larger than the subtended angle of the neutron counter. We estimate that the present absolute error in the Li(*p*,*n*) threshold is the same order of magnitude as its reproducibility and the difference between extrapolated and true threshold.

Figure 6 predicts that a very thin target, such as might be used for good resolution neutron work, will not give the same extrapolated threshold as a thick target. We mounted 10-kev and ½-kev lithium targets in the same holder and took threshold data with a proton energy resolution of 1/2000. Two thresholds were taken on each target in alternate order. Further counts on fresh target spots insured that carbon buildup was negligible. The thin-target threshold was 500 ev lower in proton energy than that of the thick target. As the Van de Graaff controls were unchanged during the runs, the reproducibility of the data was better than 100 ev.

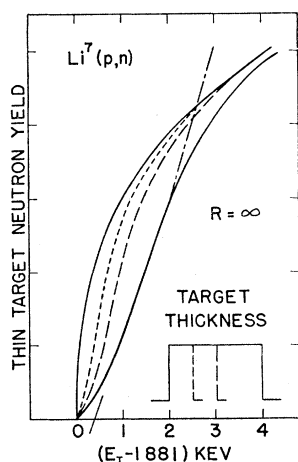


FIG. 7. Calculated modifications of the total yield of Li⁷(*p*,*n*) with no incident beam energy spread and various target thicknesses.

¹⁷ Herring, Douglas, Silverstein, and Ren Chiba, Phys. Rev. 100, 1239(A) (1955).

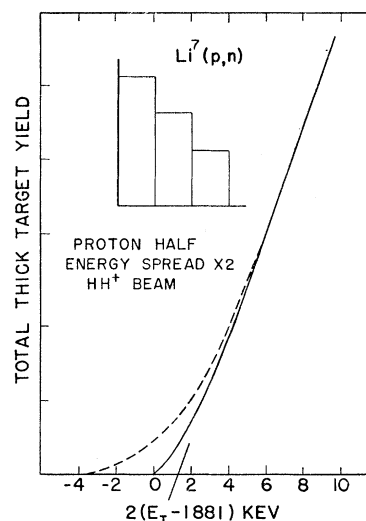


FIG. 8. Calculated modification of the Li⁷(*p*,*n*) thick-target yield due to a proton energy spread approximating the Doppler spread caused by internal motion in the HH⁺ beam.

When a threshold is measured on a very thin target, comparable in thickness to the Doppler effect, it is often convenient to define the true threshold as that of a proton of average energy which has penetrated halfway through the target, since it is the energy above this threshold which determines the average neutron energy in any direction. In fitting the data in Fig. 2 to Eq. (1), the position of this threshold was taken to be the energy of maximum slope of the experimental curve.

CONCLUSIONS

Data on Li⁷+*p* suggest levels in Be⁸ having the following descriptions: $E_0 \approx 1.9$ Mev, $1.5 > \Gamma_p > 0.5$ Mev, $(\gamma_n^2/\gamma_p^2) = 4.5$, $\gamma_n^2 > \frac{1}{3}$ the Wigner limit, $l_p = 0$, $J^\pi = 2^-$; $E_0 = 2.25$ Mev, $2\Gamma_n = 2\Gamma_p = \Gamma = 0.22$ Mev, $(\gamma_n^2/\gamma_p^2) = 5.5$, $l_p = 1$, $J^\pi = 3^+$; and $E_0 \approx 2.1$ Mev, $\Gamma \approx 0.4$ Mev, $l_p = 2$ or (1) , $J^\pi = 3^-$ or (3^+) , $\Gamma_n/\Gamma_p \ll 1$. A fourth level $E_0 \approx 3$ Mev and $J^\pi = 1^\pm$ is also suggested. The 2.1-Mev level does not appear to have an appreciable neutron or inelastic proton partial width. The suggested spin and parity assignment for the 2.1-Mev level is based on qualitative information from a number of reactions and should be treated as "tentative." (One should review the history of the 478-kev Li⁷ level to appreciate the meaning of the word "tentative.") The 1.88- and the 2.25-Mev levels give a very good quantitative fit to Li⁷(*p*,*n*) and the Be⁷(*n*,*p*) data up to 2.35 Mev. Although it cannot be claimed that these levels completely describe this region of excitation of Be⁸, they should be useful in efforts to fit more sensitive data, such as proton elastic scattering and proton and neutron polarization data. The apparent inequality of neutron and proton reduced widths for the 2⁻ and 3⁺ levels is certainly contrary to what might be expected, but it is not obvious that this inequality is in direct contradiction to the idea of charge independence of nuclear forces. We also wish to point out that the presence of an

anomaly in a reaction cross section at the threshold energy of a competing reaction may yield useful qualitative information.

One of the most interesting features of our data is the excellent empirical fit of the $\text{Li}(p,n)$ cross section from threshold to 1.92 Mev which permits the study of the effects of proton energy spread and target thickness on the neutron yield. One must consider these energy spreads if the true reaction threshold (and therefore the neutron energy) is to be known to better than about $\frac{1}{2}$

keV. We also wish to emphasize the fact that the proton energy calibration point at 1.8811 ± 0.0005 Mev¹⁶ is an extrapolated threshold taken with a target thicker than the 9-keV interval of extrapolation.

We would like to thank Dr. R. K. Adair and Dr. R. L. Macklin for unpublished communications and Professor Eugen Merzbacher for a number of very helpful discussions. We are indebted to Mr. P. Bevington and Dr. H. W. Lewis for the use of their unpublished data in the corrections on Fig. 3.

Center-of-Gravity Theorem in Nuclear Spectroscopy*

R. D. LAWSON† AND J. L. URETSKY

Physics Department and Radiation Laboratory, University of California, Berkeley, California

(Received August 5, 1957)

The j - j coupling shell model implies the existence of certain geometrical relations among the spectra of neighboring nuclei. We have considered one such relationship between states of a nucleus that is one proton or neutron away from a closed shell with states of the corresponding closed-shell nucleus. Use of this relationship has enabled us to predict excited-state spins for several nuclei, most of which are in the vicinity of mass number 60. In two cases we predict the existence of states that have not been observed.

I. INTRODUCTION

IT has recently been observed that the j - j coupling shell model implies the existence of certain geometrical relationships among the binding energies and excited states of neighboring nuclides.¹ Such relationships have been useful in the study of the ground- and excited-state properties of nuclei that could be characterized, to a good approximation, by pure (j - j coupled) nucleon configurations. In this paper we discuss a simple theorem relating the excitation spectra of certain nuclide pairs for which the limitation to pure configurations need no longer hold.

We consider a nucleus such that one kind of nucleon, say the protons, has a closed-shell configuration. The configuration of the neutrons is to be completely arbitrary. For such a nucleus we expect to find a set of energy levels corresponding to the different possible total angular momenta to which the neutron configuration can couple. The excitation energy of any such level is given by

$$\Delta E_{J_i} = \langle (j)^{2j+1} J_i | V | (j)^{2j+1} J_i \rangle - \langle (j)^{2j+1} J_0 | V | (j)^{2j+1} J_0 \rangle. \quad (1)$$

* Work supported by U. S. Atomic Energy Commission and U. S. Army Office of Ordnance Research.

† Now at the Enrico Fermi Institute for Nuclear Studies, University of Chicago, Chicago, Illinois.

¹ I. Talmi and R. Thieberger, *Phys. Rev.* **103**, 718 (1956); S. Goldstein and I. Talmi, *Phys. Rev.* **102**, 589 (1956); **105**, 995 (1957); I. Talmi, *Phys. Rev.* **107**, 1601 (1957); R. D. Lawson and J. L. Uretsky, *Phys. Rev.* **106**, 1369 (1957). The idea of exploiting geometrical relations among the energies of many particle systems was first applied to atomic spectroscopy by R. F. Bacher and S. Goudsmit, *Phys. Rev.* **46**, 948 (1934).

The state vectors in this expression exhibit explicitly the last proton closed shell (or subshell), which is trivially vector-coupled to the neutron angular momentum. We denote the ground-state neutron angular momentum by J_0 , and V denotes the sum of the two-body interaction terms.

Let us now split off one proton from the closed shell (the appropriate fractional parentage coefficient is unity) and recouple the single proton to the neutrons in order to form a new angular momentum J_3 . J_3 is then vector-coupled to the remaining $2j$ protons to form the total angular momentum J_i (or J_0). If we rewrite Eq. (1) using the new representation of the state vectors, we discover that²

$$(2j+1)\Delta E_{J_i} = (2J_i+1)^{-1} \sum_{J_3} (2J_3+1) \times \langle j J_i, J_3 | V | j J_i, J_3 \rangle - (2J_0+1)^{-1} \sum_{J_3'} (2J_3'+1) \times \langle j J_0, J_3' | V | j J_0, J_3' \rangle. \quad (2)$$

The matrix elements that appear on the right-hand side of Eq. (2) are just the first-order energies of a nucleus that differs from the one under consideration by the addition or subtraction of a single proton in state j . It is to be emphasized that the neutron states J_i and J_0 are states of the same configuration. It is clear that we are not concerned with the details of the

² This relation is readily derived from the recoupling relation for angular momenta. See Biedenharn, Blatt, and Rose, *Revs. Modern Phys.* **24**, 249 (1952).